J Mater Sci (2007) 42:5411–5415
DOI 10.1007/s10853-006-0814-0

Annealing effects on the reordering of severe plastic deformed boron doped Ni_3Al

Atef Korchef · Abdelwahab Kolsi · Nabil Njah

Received: 27 January 2006 / Accepted: 14 August 2006 / Published online: 28 March 2007

Abstract X-ray diffraction (XRD) and differential scanning calorimetry (DSC) were used to investigate the reordering process of a partially disordered $Ni_{76}Al_{24}$ (0.2 wt.%B) powder with annealing times and temperature. The long-range order parameter varied linearly with temperature and a significant ordered state was observed at 773 K. The DSC measurements showed one main exothermal peak in the temperature range of 493–913 K. The maximum rate of energy release occurred at 763 ± 2 K with a total thermal effect of $\Delta H = 52 \pm 9$ j/g. The DSC peak showed a shoulder around its maximum temperature of 763 ± 2 K which was attributed to order stabilization. The presence of boron in the alloy enhanced the transformation temperature by increasing the enthalpy of vacancies migration without affecting the reaction enthalpy.

Introduction

Intermetallic phases (Ni_3Al, Nb_3Sn, Ni_3Fe...) are used for high temperature applications. Their physical and mechanical properties at elevated temperature are more interesting than of superalloys or ceramics. In fact, intermetallics show higher strength than superalloys because atoms are strongly bonded and a lower brittleness than the modern ceramics because of the metallic bonding. However, the major problem of intermetallic alloys is their intergranular brittleness. The investigations of Aoki and Izumi [1] have shown that the ductility of polycrystalline Ni_3Al could be enhanced by addition of small diameter atoms like boron. Thus, further potential applications for Ni_3Al are developed such as heating elements, turbines, valves, etc...

Boron is known to segregate to grain boundaries where its concentration reaches 5at.%. For the off stoichiometric alloys, this concentration decreases with the increase of aluminium content. For example, the boron segregation is reduced by 45% when aluminium concentration increases from 24 to 25.2 at % [2]. On the other hand, boron occupies on the interstitial site of the body-centered position of the cubic structure of Ni_3Al alloy, since the volume of this site is large. Consequently, boron occupation induces further ordering of the constituent atoms Ni and Al [3] and probably changes the lattice parameter of Ni_3Al. Lattice parameter measurements have shown that boron is soluble in stoichiometric Ni_3Al alloy up to at least 1.12 at % and produces a lattice strain ($\Delta a/a$ 1/a) of 0.13 [4]. Moreover, the lattice parameter depends on stoichiometry since its evolution is more pronounced for stoichiometric boron doped Ni_3Al than for off-stoichiometric alloys [3]. In addition, the lattice parameter depends on third addition elements [5], rates of cooling [6, 7] and temperature of annealing [8].

At low temperature, the structure of a crystal is perfectly ordered. The rise of the temperature will gradually destroy this order. Thus, it is necessary to measure a parameter of order, which characterizes the state of the structure

A. Korchef (✉)
Technopole de Borj-Cédria,
B.P. 273, Soliman 8020, Tunisia
e-mail: atef.korchef@inrst.rnrt.tn

A. Kolsi
Laboratoire de Chimie Inorganique, Faculté des Sciences de Sfax, Sfax 3018, Tunisia

N. Njah
Laboratoire de Métallurgie Appliquée, Faculté des Sciences de Sfax, Sfax 3018, Tunisia

compared to the perfectly ordered state. In a long range ordered solid, formed of atoms A and B, one classify the reticular sites in two families α and β corresponding to the positions of atoms A and B in perfectly ordered stoechiometric alloy, respectively. For example, in a structure of the type $L1_2$ (Cu_3Au, Ni_3Al...), the α sites are the corners of the cube and the β sites are the centers of the faces. By admitting that the probability of occupation of a site is independent of the arrangement of the atoms on the other site and that there is no correlation between the probability of occupation of two close sites, Bragg-Williams [8] characterized the state of order of a binary system A–B by the long range order parameter (LRO), S, which is given by the expression [9]:

$$S = \frac{C_A^{\alpha} - C_A}{1 - C_A} = \frac{C_B^{\beta} - C_B}{1 - C_B} \quad (1)$$

with $(C_A)^{\alpha}$ the fraction of the sites occupied by atoms A; $(C_B)^{\beta}$ the fraction of the sites occupied by atoms B; C_A and C_B are the atomic fractions of A and B in the alloy, respectively with $C_A + C_B = 1$ for the completely ordered state (S = 1) defined by the occupation of all the sites α by atoms A and all the sites β by atoms B. The completely disordered state (S = 0) depends on the structure of the compound. For a compound AB_3, it corresponds to $(C_A)^{\alpha} = C_A = 0.25$ i.e. 25% of the sites α remain occupied by atoms A, whereas for a compound AB of B_2 structure (CsCl type structure) it corresponds to $(C_A)^{\alpha} = C_A = 0.5$.

When an ordered undoped or boron-containing Ni_3Al alloys are subjected to plastic strain, caused such by ball-milling [10, 11], cold rolling [12], filling [13, 14] and irradiation [15, 16], the order is partially or completely destroyed. For example, Jang and Koch [10] have shown that for an annealing at 800 °C, the long-range order (LRO) parameter, S, of Ni_3Al was 0.96. After ball-milling for 5 h and more, the LRO was entirely destroyed (S = 0). Ball et al. [17] have observed that the LRO parameter of $Ni_{76}Al_{24}$ (0.24 at % boron) decreased continuously from 1 to 0.2 when the sample was cold-rolled to reductions of 10 and 95%, respectively.

In the present work, X-ray diffraction (XRD) analysis and differential scanning calorimetry (DSC) were used to investigate the evolution of the recovery process of $Ni_{76}Al_{24}$ + 0.2 wt.%B with annealing time and temperature up to 773 K in a step of 100 K. The effect of boron addition on the reordering process of Ni_3Al alloy was studied.

Material and experimental procedures

The intermetallic alloy used in this work was a boron doped $Ni_{76}Al_{24}$ (0.2 wt.%B) material. The chemical composition of the alloy is given in Table 1. Liu et al. [2] have shown that the solubility of boron was greater than 0.2 wt.% in Ni_3Al with 24 at.% Al. Thus, the added boron should be in solid solution. The alloy was prepared by melting together weighed quantities of high purity Ni, Al and Ni-18 wt.%B master alloy in an inductive plasma furnace. The $Ni_{76}Al_{24}$ (0.2 wt.%B) alloy was homogeneized by annealing for 40 h at 1323 K under a vacuum of 6 10^{-4} Pa followed by furnace cooling. Thereafter, the alloy was cold-rolled to a reduction of 50% and powder from the alloy was obtained by machining. Then, the powder was sealed in silica tube and subjected to isothermal anneals of 5, 10, 20, and 40 h at 489 K and to isochronal 5 h anneals at intervals of 100 K over the temperature range of 573–773 K. All anneals were carried out under argon atmosphere. After each anneal, the powder was furnace cooled.

Differential scanning calorimetry (DSC) measurements were performed with a Perkin Elmer calorimeter. The powder was heated in closed copper crucibles with a heating rate of 40 K/min. Three heating runs were performed under argon atmosphere on the same sample up to 1123 K. The two last runs were used to determine the baseline.

X-ray diffraction (XRD) was carried out using a nickel-filtered Cu-Kα radiation. The XRD patterns were recorded at room temperature with a scan rate of 5×10^{-3} deg/s in the scanning range 2θ = 30–80°.

The long range (LRO) parameter, S, was calculated from the integrated intensity ratio I_f/I_s of the fundamental to superlattice XRD peaks, according to the relationship [9]:

$$S^2 = \frac{I_s |F_f|^2 (L_p)_f (e^{-2M})_f (m)_f}{I_f |F_s|^2 (L_p)_s (e^{-2M})_s (m)_s} \quad (2)$$

where I is the measured integrated intensity, F is the structural factor, Lp is the Lorentz polarisation factor $(1 + \cos^2(2\theta)/\sin^2\theta\cos\theta)$, $(\exp(-2M))$ is the temperature factor and m is the multiplicity factor. The subscripts s and f refer to superlattice and fundamental XRD peaks, respectively. The area under each peak was measured three times using 'Winploter' software and the average of these measurements was taken as a measure of the integrated intensity of the profile. The values of the structural factors were calculated from the scattering factors of Ni and Al with respect to the $L1_2$ structure of Ni_3Al. These scattering

Table 1 Alloy composition

Alloy	Ni (at.%)	Al (at.%)	Boron (wt.%)
$Ni_{76}Al_{24}$ (0.2 wt.%B)	76.03 *	23.97 *	0.202

*Referred to (Ni + Al)

factors were obtained from the international table of crystallography [18]. The value of the Debye-Waller factor, M, was calculated from the amplitude of vibration $\langle\mu\rangle$ for the Ni_3Al structure according to the relationship $M = B \sin^2\theta/\lambda^2$ where $B = 8\pi^2 \langle\mu^2\rangle/3 = 0.00835$ nm^2 [13]. In the present work, the order parameter was estimated from the pairs of XRD peaks (110) and (220). The error was lower than 5% of the S value.

Results and discussion

The XRD patterns of $Ni_{76}Al_{24}$ (0.2 wt.%B) for selected annealing times at 489 K and for 5 h anneal at 773 K are presented in Fig. 1. For all annealing times at 489 K, only the (110) superlattice XRD peak was observed with a very low intensity compared to those of fundamental peaks (Fig. 1a). This indicates a partially disordered state of the $Ni_{76}Al_{24}$ (0.2 wt.%B) powder. This state was not affected by the isothermal anneals carried out up to 40 h. After a cold-rolling at a reduction of 50% and machining, the alloy was partially disordered, so that the deformations were lower than to reach a fully disordered structure. The disorder created at low deformations was probably partially removed by annihilation of dislocations with the same Burger vector. In addition, the powder exhibited relatively broad diffraction lines due to enhanced lattice distortions and/or grain refinement [19]. A slight shift towards lower angles of the fundamental peaks (for example the (111) peak) was observed at 489 K (figure 1b). This may be related to relaxation processes of compressive stresses caused by cold rolling and machining of the alloy to obtain the powder. For anneals up to 673 K, no significant change in the XRD patterns was observed. At 773 K, all the superlattice peaks (110), (210) and (211) appeared with appreciable intensities in the range scan of 30–80° (Fig. 1c). This indicates a significant reordering of the alloy. The peak profiles became less broad than the deformed alloy. This is due to the decrease of the lattice distortions and to grain size increase [19]. Also, a peak shift to higher angles was observed (Fig. 1d), which indicate a slight decrease of the lattice parameter with annealing temperature. In fact, after deformation of the alloy, the lattice parameter, calculated from a linear regression analysis using the Nilson–Reley function [20], was 3.5848 Å and decreased to 3.5616 Å after an anneal of 5 h at 773 K. The decrease of the lattice parameter was probably due to the presence of stacking faults in the alloy. In fact, after annealing, the stacking faults were faulted loops with the emission of vacancies as showed by Wagner and Helion [21]. These vacancies diffuse through the lattice alloy producing a decrease of the dislocation concentration. Consequently, the crystalline alloy rearranged into more stable and compact configuration, which leads to the decrease of the lattice parameter. In this work, the vacancies concentration was probably low since the alloy was not rapidly cooled, so the decrease of the lattice parameter, a, was rather weak, i.e. $\Delta a/a = 0.0064$.

The evolution of the LRO parameter, S, with temperature is given in Fig. 2. The S-values were calculated using Eq. (2). Note that the S value of the as deformed alloy was not reported in Fig. 2 because it was comparable to that at

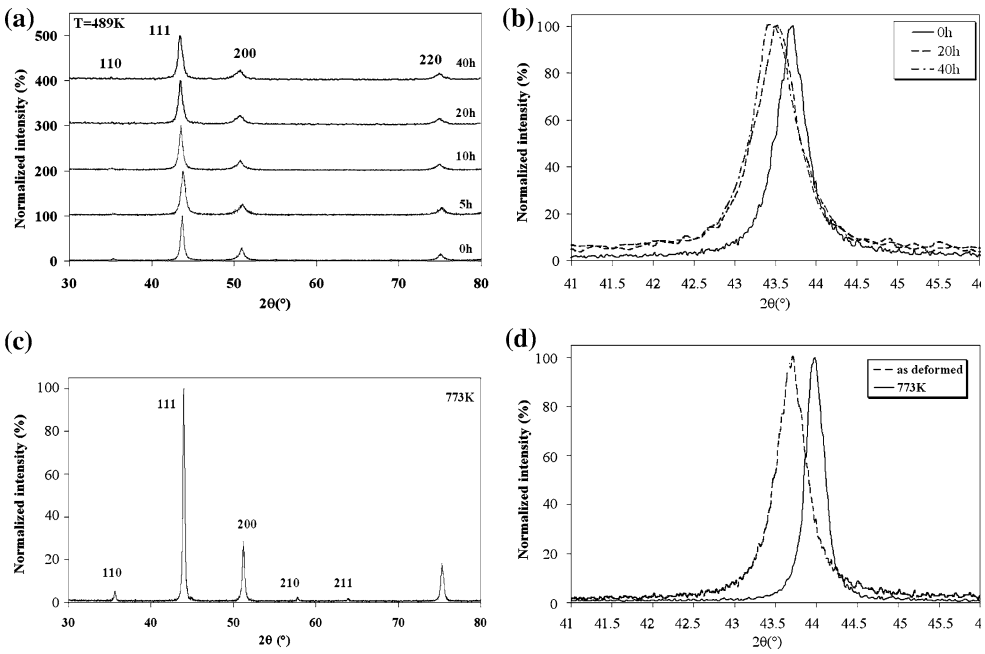

Fig. 1 (**a**) XRD patterns and (**b**) the (111) peak profile for different annealing times at 489 K, (**c**) XRD pattern at 773 K and (**d**) the (111) peak profile at 773 K compared to that of the deformed alloy

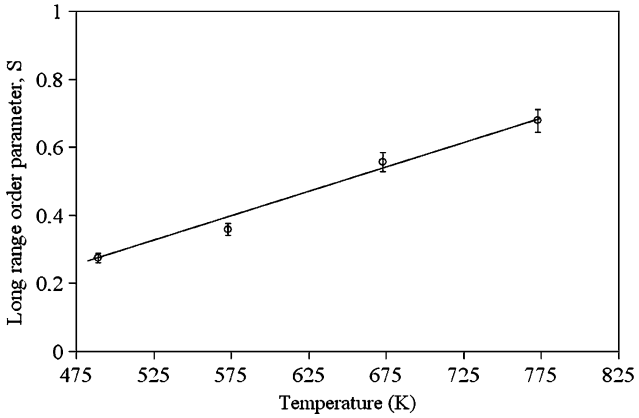

Fig. 2 Evolution of the long range order parameter, S, with temperature

489 K. S increased linearly with the temperature from 0.27 at 489 K to 0.67 at 773 K. In the present work, the S value did not reach the theoretical value (S = 1). Also, despite the enhanced annealing temperature of 1173 K used in reference [13], S (= 0.96) remained lower than 1. This is due to the presence of faults and impurities in the sample. Indeed, they prevent the achievement of the order recovery process to reach the full ordered state.

The DSC measurements are shown in Fig. 3. Three heating runs were performed: one run was conducted on the sample up to 973 K. On repeating two successive heating runs on the same sample, no transformation was detected, indicating an irreversible transformation. The last heating run was used to determine the base line. DSC results show that the alloy exhibited one main exothermal peak in the temperature range of 493–1013 K. The maximum rate of energy release occurred at 763 ± 2 K with a total thermal effect of ΔH = 52 ± 9 j/g. This enthalpy value was obtained from the integrated peak area between the baseline and the DSC curve of the tested sample. The DSC curve shows a shoulder in the temperature range of 723–

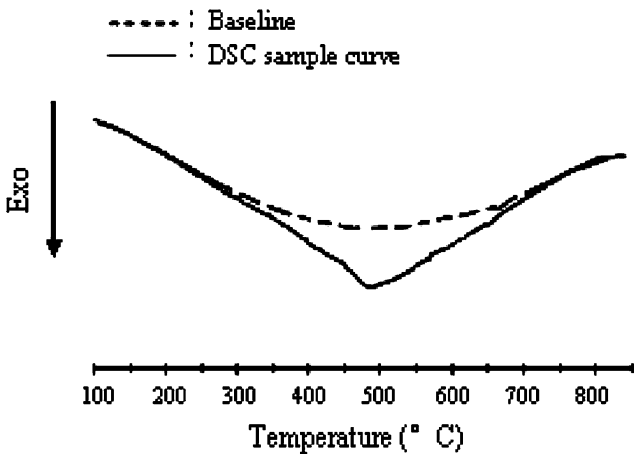

Fig. 3 DSC curve of the $Ni_{76}Al_{24}$ (0.2 wt.%B) deformed alloy

823 K indicating probably an additional exothermal contribution. Baro et al. [22] have observed a complex calirometric signal for an intermetallic atomized powder of Ni-23.3 at.%Al + 1000 ppm B. In their work, isothermal anneals coupled with further continuous heating experiments, which allowed the effect of the annealing to be checked, were performed. Three stages were identified: the first one at low temperature did not involve any change in the LRO parameter. Harris et al. [23] have attributed this stage to the reestablishment of short-range order. The second stage observed in the range temperature of 500–700 K was associated with the simultaneous evolution of the ordered phase. This stage can be compared to the one obtained in the present work. Finally, a third stage detected at high temperature was attributed to the annealing out of dislocations not mobile at temperature as low as those of the first and second stages. In this study, the evolution of the XRD patterns with temperature showed that all superlattice peaks appeared for annealing at 773 K. Thus, the reestablishment of the LRO is significant at this temperature. Therefore, the additional contribution mentioned above in the DSC measurement, is due to the order recovery of the alloy. The heat flow in the DSC experiment is related to the ordering reaction and the recovery or recrystallization processes. However, it was shown that the ordering energy was very low [14, 24] so the recovery or recrystallization processes significantly contribute to the heat flow recorded in DSC. This is confirmed by the decrease of the peak profile broadening at 773 K in XRD analysis.

Korznikov et al. [25] have investigated the thermal evolution of high purity and boron doped submicrocrystalline Ni_3Al produced by severe plastic deformation. Their DSC measurements showed a main exothermal peak in both materials, which was attributed to the release of stored energy of cold work. Table 2 gives their DSC results compared to those obtained in the present work. It is noticeable, from this table, that the temperature of order recovery of $Ni_{76}Al_{24}$ (0.2 wt.%B) is greater than those of the undoped and 0.1 wt.% boron dopped alloys, while the enthalpy values are comparable. This is due to the highest boron concentration in the alloy used in this work. Thus,

Table 2 DSC results of undoped and boron-doped Ni_3Al alloys

Alloy	Deformation method	T (K)	ΔH (j/g)	Reference
Ni-25Al	Torsion under high pressure	618 ± 2	–48 ± 2	[25]
Ni-23, 7Al (0,1% pds B)	Torsion under high pressure	717 ± 2	–46 ± 8	[25]
Ni-23,97Al (0,2% pds B)	Cold-rolling + machining	763 ± 2	–52 ± 9	Present work

boron addition enhanced the transformation temperature by increasing the enthalpy of vacancies migration without affecting the reaction enthalpy. This result is comparable to previous irradiation experiments, which showed that boron slowed down the reordering processes by increasing the migration enthalpy of vacancies due to boron addition [15].

Conclusion

Intermetallic materials are potential candidates for enhanced temperature applications. Their high temperature properties (i.e. high elastic moduli, high melting temperature and low atomic mobility) are of a large interest. X-ray diffraction (XRD) analysis and differential scanning calorimetry (DSC) were used to investigate the lattice parameter and the long-range order (LRO) evolutions of $Ni_{76}Al_{24}$ + 0.2 wt.%B with annealing time and temperature. The boron doped material was subjected to a subsequent cold-rolling and machining in order to obtain powders and hence to disorder the sample. For increasing annealing time, the lattice parameter decreases for annealing time above 10 h at 498 K. This is due to presence of stacking faults in the alloy. The LRO parameter, obtained by comparison of integrated intensities of fundamental and superlattice XRD peaks, increases linearly with temperature. The DSC results showed a large exothermal peak. The corresponding enthalpy was equal to 52 ± 9 j/g. The DSC peak showed a shoulder around its maximum temperature of 763 ± 2 K. This peak was attributed to order stabilization. The presence of boron in the alloy increased the transformation temperature by increasing the enthalpy vacancies migration without affecting the reaction enthalpy.

References

1. Aoki K, Izumi O (1979) J Japan Inst Metals 43:1190
2. Liu CT, White CL, Horton JA (1985) Acta Metall 33:213
3. Takasugi T, Masahashi N, Izumi O (1985) Acta Metall 33:1259
4. Baker I, Huang B, Schulson EM (1988) Acta Metall 36(3):493
5. Briant CL, Huang SC (1986) Metall Trans A 17A:2084
6. Pearson D (1958) A Handbook of lattice spacings, vol 1. Pergamon Press, Oxford
7. Kim YG, Yoon GW, Stoloff NS (1985) J Mater Sci 4:1407
8. Bragg WL, Williams EJ (1934) Proc Roy Soc A 145:699
9. Ramesh R, Vasudevan R, Pathiraj B, Kolster BH (1992) J Mater Sci 27:270
10. Jang JSC, Koch CC, Mar (1990) J Mater Res 5:3
11. Khitouni M, Kolsi AW, Njah N (2003) Ann Chim Sci Mater 28:17
12. Mohan Rao PV, Satyanarayana Murthy K, Suryanarayana SV, Nagender Naidu SV (1992) Scripta Met Mater 27:1085
13. Mohan Rao PV, Satyanarayana Murthy K, Suryanarayana SV, Nagender Naidu SV (1993) J Appl Cryst 26:670
14. Khitouni M, Njah N, Gilbon D (2004) Scripta Mater 50:77
15. Njah N, Gilbon D, Dimitrov O (1995) Scripta Metallur Mater 33(9):1379
16. Njah N, Kolsi AW (1999) Ann Chim Sci Mat 24:145
17. Ball J, Mitteau R, Gottstein G, (1991) European Workshop on ordering and disordering, July 10–12, Grenoble
18. ''International Table for X-Ray Cristallography'' (1962) vol 11. Kynoch Press, Birmingham, p 201
19. Kuschke WM, Keller RM, Grahl P, Mason R, Arzt E (1995) Z Metallkdr 86:12
20. Azàroff LV, Buerger M (1958) The powder Method, Mc Grow_Hill, New York, 238
21. Wagner CNJ, Helion JC (1965) J Appl Phys 36:2830
22. Baro MD, Surinach S, Malagelada J, Clavagura-Mora MT, Gialanella S, Cahn RW (1993) Acta Mater 41(4):1065–1073
23. Harris SR, Pearson DH, Garland CM, Fultz B (1991) J Mater Res 6:2019
24. Masahashi N, Takasugi T, Izumi O (1988) Acta Met 36:1815
25. Korznikov AV, Dimitrov O, Korznikova GF, Dallas JP, Idrisova BSR, Valiev RZ, Faudot F (1999) Acta Mater 47:3301